Activation of NMDA receptors increases proliferation and differentiation of hippocampal neural progenitor cells

Jae-Yeol Joo[1,*,‡], Byung-Woo Kim[1,2,‡], Jeong-Sik Lee[1,2,‡], Jin-Yong Park[1], Sunoh Kim[3], Young-Joo Yun[1], Sang-Hun Lee[4], Suk-Ho Lee[4], Hyewhon Rhim[3] and Hyeon Son[1,2,§]

[1]Department of Biochemistry and Molecular Biology, and [2]BK21, Hanyang University College of Medicine, 17 Haengdang-dong, Sungdong-gu, Seoul 133-791, Korea
[3]Biomedical Research Center, Korea Institute of Science and Technology (KIST), 39-1 Hawholgok-dong Sungbuk-gu, Seoul 136-791, South Korea
[4]Cell Physiology Laboratory, Department of Physiology, Seoul National University College of Medicine, 28 Yongon-Dong, Chongno-gu, Seoul 110-799, Korea

*Present address: Department of Molecular Neurobiology and Pharmacology, Graduate School of Medicine, University of Tokyo, Tokyo 113-0033, Japan
‡These authors contributed equally to this work
§Author for correspondence (e-mail: hyeonson@hanyang.ac.kr)

Accepted 4 February 2007
Journal of Cell Science 120, 1358-1370 Published by The Company of Biologists 2007
doi:10.1242/jcs.002154

Summary

The prolonged effects of *N*-methyl-*D*-aspartate (NMDA) receptor activation on the proliferation and differentiation of hippocampal neural progenitor cells (NPCs) were studied. Under conditions of mitogen-mediated proliferation, a single NMDA pulse (5 μM) increased the fraction of 5-bromo-2-deoxyuridine (BrdU)-positive ($BrdU^+$) cells after a delay of 72 hours. Similarly, a single systemic injection of NMDA (100 mg/kg) increased the number of $BrdU^+$ cells in the dentate gyrus (DG) after 28 days, but not after 3 days. NMDA receptor activation induced an immediate influx of Ca^{2+} into the NPCs and the NPCs expressed and released vascular endothelial growth factor (VEGF) in an NMDA receptor-dependent manner within 72 hours. With repetitive stimulation at the same dose, NMDA stimulated the acquisition of a neuronal phenotype accompanied by an increase in the expression of proneural basic helix-loop-helix (bHLH) factors. Together these findings suggest that neurogenesis in the developing brain is likely to be both directly and indirectly regulated by complex interactions between Ca^{2+} influx and excitation-releasable cytokines, even at mild levels of excitation. In addition, our results are the first to show that stimulation of NPCs may lead to either proliferation or neuronal differentiation, depending on the level of NMDA receptor activation.

Supplementary material available online at
http://jcs.biologists.org/cgi/content/full/120/8/1358/DC1

Key words: Rat, Hippocampus, NMDA, Ca^{2+}, Progenitors

Introduction

Neuronal activity is primarily generated by neurotransmitters and the role of neurotransmitters also extends to proliferation and neuronal differentiation (Levitt et al., 1997). Glutamate, the major excitatory neurotransmitter, is important for migration, differentiation and neuritogenesis of neurons (Simon et al., 1992; Rakic and Komuro, 1995). The role of glutamate receptor activation in neural development is complex. Whereas members of the α-amino-3-hydroxy-5-methyl-4-isoxazolepropionic acid (AMPA) and kainate (KA) subclass of ionotropic glutamate receptor antagonists increase the proliferation of neocortical progenitors (Cameron et al., 1995; Cameron et al., 1998), activation of the *N*-methyl-*D*-aspartate (NMDA) (but not the AMPA-KA) receptor is required for the proliferation of embryonic striatal progenitors (Luk et al., 2003). There is now evidence that neural activity can play neurogenic roles in the adult brain in addition to its role in neural development. Activation of NMDA receptors on proliferating progenitors induces neuronal differentiation of adult-derived neural progenitor cells (NPCs) in vitro (Deisseroth et al., 2004). Similarly an increase of intracellular Ca^{2+} ($[Ca^{2+}]_i$) induced by γ-aminobutyric acid (GABA) receptor activation promotes neurogenesis in adult hippocampal NPCs of the intact brain (Tozuka et al., 2005).

The complexity of the neurochemical scenario involving NMDA receptors is even greater in the context of neural activity levels. Pharmacological blockade of NMDA receptors by antagonists increases proliferation in the hippocampus (Nacher and McEwen, 2006). By contrast, NMDA blockers inhibit seizure- and stroke-induced proliferation of NPCs in the hippocampus (Arvidsson et al., 2001). It was therefore of interest to address the mechanisms that produce these contrasting effects, and we have tested whether the inconsistent results are related to secondary effects due to the fact that NPCs can produce a variety of factors following NMDA receptor activation.

The contradictory findings could also be due to the ability of agonists/antagonists to affect different cell types in the intact brain. In the intact brain, a systemic injection of NMDA receptor blockers may affect many more types of neurons than local stimulation achieved by physiological neural activity. Therefore, it is important to use a simplified assay system.

In the present study, we aimed to address the hypothesis that neural activity causes depolarization, and that this evokes a depolarization-dependent cascade leading to the production of a number of factors and an increase of neurogenesis. We examined the effects of NMDA on the proliferation and differentiation of embryonic hippocampal NPCs. We chose a relatively prolonged stimulus paradigm – because this is necessary to induce de novo protein synthesis – and non-excitotoxic, low concentrations of NMDA because of their prolonged application.

Results

NMDA receptor activation promotes the proliferation of hippocampal NPCs in vitro

To control accurately the extent of activation, and determine the detailed molecular mechanisms responsible for NMDA receptor-dependent neurogenesis, we used well-characterized primary cultures of proliferating cells isolated directly from the hippocampi of embryonic day (E)16.5 rats. These cells have the ability to proliferate in the presence of basic fibroblast growth factor (bFGF), and differentiate into neurons or glial cells after withdrawal of bFGF (Kim et al., 2004). If neurotransmitters play a role as local environmental factors in regulating neurogenesis in the intact brain, they are presumably present at non-apoptotic levels for prolonged periods. Therefore, to mimic persistent neural activity we applied low to medium stimuli for 1-3 days – a longer period than previously employed (LoTurco et al., 1995). We found that the treatment of proliferating NPCs with various concentrations (0.5-20 μM) of NMDA for 3 consecutive days reduced 5-bromo-2-deoxyuridine (BrdU) incorporation, and induced cell death (see supplementary material Fig. S1A-C).

To investigate whether NMDA-mediated glutamatergic mechanisms influence cell proliferation when applied at lower levels that do not cause excitotoxicity, cells that had been kept 6 days in vitro (DIV) were incubated with a single pulse of NMDA (5 μM) for 24 hours followed by BrdU treatment and fixation 24 hours (7 DIV), 48 hours (8 DIV) or 72 hours (9 DIV) after the stimulation. Cells treated with NMDA and fixed 24 hours or 48 hours later did not show an increased proportion of BrdU-positive ($BrdU^+$) cells (supplementary material Fig. S1D). However, there was a significant increase in the proportion of $BrdU^+$ cells 72 hours after treatment (Fig. 1B,C: control, 36.8±3.5; NMDA 1', 52.4±8.7, $P<0.01$). A single pulse of NMDA at <2 μM had no effects on the proportion of $BrdU^+$ cells (data not shown), and repeated exposure to 5 μM NMDA for 2 or 3 consecutive days did not increase the percentage of $BrdU^+$ nuclei (0 and –63% of control, respectively), possibly due to excitotoxicity (Fig. 1A,B and supplementary material Fig. S1E). Single pulses of higher concentrations (>10 μM) of NMDA for 1 day gradually decreased the proportion of $BrdU^+$ nuclei, in accordance with the expected excitotoxic effects (data not shown). A single pulse of NMDA (24 hours at 5 μM) was used in all subsequent experiments. To confirm the involvement of functional NMDA receptor channels in proliferation, we added an NMDA

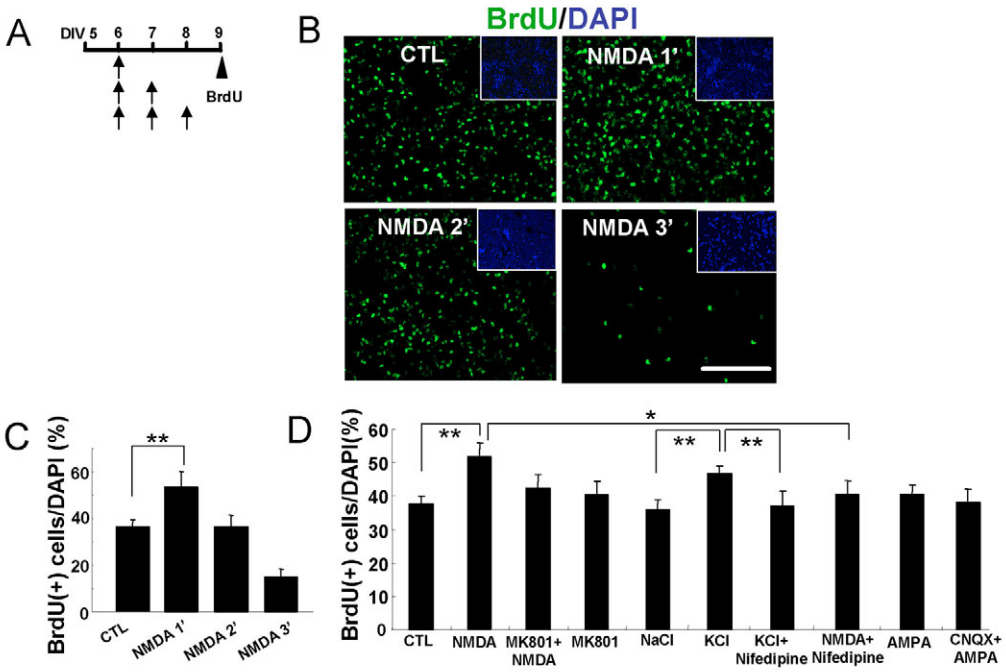

Fig. 1. BrdU incorporation increases after a delay in proliferating hippocampal NPCs following a single 24-hour pulse (but not repetitive pulses) of NMDA. (A) Diagram illustrating experimental procedures. (B) Micrographs of cells comparing of BrdU incorporation following treatment with a single pulse of NMDA (5 μM) over 1 day (NMDA 1'), two pulses over 2 days (NMDA 2') or three pulses over 3 days (NMDA 3′) in the presence of bFGF. Cells were fixed on 9 DIV. Bar, 100 μm. (C) Graph showing BrdU incorporation in cells treated as in B; $n=8$. (D) BrdU incorporation following single pulses for 24 hours. Proliferating cells were treated with NMDA (5 μM), MK801 (5 μM), NaCl (5 mM), KCl (5 mM), AMPA (5 μM), or CNQX (10 μM). The percentage of $BrdU^+$ cells [BrdU (+)] is shown. Insets, All the cells were counterstained with DAPI (blue), and total and $BrdU^+$ cells were counted with a microscope in ten non-overlapping fields per well. Each value represents the mean ± s.e.m. of eight (B,C) and four (D) independent experiments. CTL, control; $*P<0.05$,$**P<0.01$, $***P<0.001$.

receptor antagonist MK801 (5 μM) 30 minutes before exposing cells to NMDA. This prevented the increase in number of $BrdU^+$ cells, whereas MK801 alone had no effect (Fig. 1D: CTL vs MK801+NMDA, 40.7±4.3, $P>0.05$), suggesting that proliferation of NPCs is, at least in part, dependent upon NMDA receptor activity and that mild activation of NMDA receptors is necessary to provoke DNA synthesis in a sub-population of proliferating NPCs. In addition, the delayed effect of NMDA on the proportion of $BrdU^+$ cells suggests that NMDA receptor activation may provoke responses that do not have an immediate effect.

To investigate the possibility that excitatory stimulation via NMDA receptors stimulates proliferation by causing membrane depolarization followed by Ca^{2+} influx we first tested whether depolarization alone was capable of eliciting similar mitogenic effects. The application of 5 mM KCl (a previously reported non-toxic dose) (Son et al., 2003), increased the fraction of $BrdU^+$ cells (Fig. 1D: NaCl, 36.6±2.4; KCl, 46.7±2.0, $P<0.01$), suggesting that voltage-gated Ca^{2+} channels (VACCs) are activated by KCl in the NPCs. Since NMDA- and KCl-induced depolarization led to an increase in $[Ca^{2+}]_i$, it seemed possible that the increased DNA synthesis was also due to increased Ca^{2+} influx into the NPCs through VACCs as well as NMDA-receptor-mediated Ca^{2+} channels. To test whether the KCl-induced increase in $BrdU^+$ cells involves Ca^{2+} influx through L-type Ca^{2+} channels, we applied nifedipine (3 μM), an L-type Ca^{2+} channel antagonist, which indeed blocked the KCl-induced increase in the number of $BrdU^+$ cells (Fig. 1D: KCl, 46.7±2.0; KCl+Nifedipine, 37.8±4.5, $P<0.05$). Nifedipine also blocked the NMDA-induced increase in the fraction of $BrdU^+$ cells, indicating that NMDA-dependent increase in $BrdU^+$ cells, at least partially, involves Ca^{2+} influx through L-type Ca^{2+} channels (Fig. 1D). Similar cultures were exposed to 6-cyano-7-nitroquinoxaline-2,3-dione (CNQX) in order to compare NMDA with AMPA-receptor-mediated and KA-receptor-mediated effects, but no significant change in BrdU uptake was observed ($P>0.05$). These results suggest that depolarizing stimuli contribute to DNA synthesis during proliferation primarily by Ca^{2+} influx.

Effects of depolarization and NMDA on $[Ca^{2+}]_i$ in hippocampal NPCs

In order to detect any increase in $[Ca^{2+}]_i$ following stimulation with either KCl or NMDA we used fura-2-based digital imaging (Fig. 2A). Owing to the fact that embryonic cells express relatively few ion channels and receptors (LoTurco et al., 1995; Cai et al., 2004) small, transmitter-induced $[Ca^{2+}]_i$ transients are discussed to be a general feature of embryonic cells. Thus, to clearly demonstrate the existence and functionality of Ca^{2+} channels in proliferating NPCs, higher concentrations of KCl and NMDA than those used for long-term application were used. Exposure of proliferating NPCs to KCl (50 mM) or NMDA (100 μM) for 10 seconds resulted in an immediate increase in $[Ca^{2+}]_i$ that returned slowly to baseline following removal of the KCl or NMDA (Fig. 2A). This indicates that functional Ca^{2+} channels are expressed and activation of responsive Ca^{2+} channels (signaling) leads to elevated $[Ca^{2+}]_i$ within the proliferating NPCs. Having obtained evidence that functional channels required for KCl or NMDA responses exist, we questioned whether low concentrations of KCl or NMDA induce Ca^{2+} influx at different kinetics compared with those induced by high concentrations. We therefore monitored $[Ca^{2+}]_i$ with continuous application of KCl in a solution that contained 2.5 mM Ca^{2+} and 1 mM Mg^{2+} (see legend Fig. 2A). Treatment with 5 mM KCl caused a $[Ca^{2+}]_i$ elevation, which gradually increased with time (Fig. 2B; 50 cells of 50 observed cells). The simplest explanation for these results is that 5 mM KCl causes a progressive influx of Ca^{2+} from extracellular buffer, thereby directly causing a $[Ca^{2+}]_i$ rise, which in turn is responsible for maintaining a long-lasting $[Ca^{2+}]_i$ plateau. To identify the origin of the KCl-induced Ca^{2+} influx we examined whether these signals are associated with influx of extracellular Ca^{2+}. We tested this question in cells to which KCl was added in a Ca^{2+}-free buffer containing EGTA. Perfusing cells with Ca^{2+}-free buffer completely blocked the KCl-induced Ca^{2+}-response. Similar observations were made in cells treated with 5 μM NMDA by using Ca^{2+}-containing or Ca^{2+}-free buffer (Fig. 2B; 50 cells of 50 observed cells), indicating that the Ca^{2+} response mediated by KCl (5 mM) or NMDA (5 μM) in proliferating NPCs is largely due to influx of extracellular Ca^{2+}.

To test whether L-type Ca^{2+} channels are present and play a role in this Ca^{2+} influx, whole-cell Ba^{2+} currents were recorded using patch-clamp methods. We detected microscopic Ba^{2+} currents in cells subjected to depolarizing step pulses (Fig. 2Ca). Ba^{2+} currents (I_{Ba}) ranging from 206-332 pA were recorded in 28.5% cells (four out of 14 cells), a ratio slightly higher than previously reported in fetal neural stem cells (NSCs) (Cai et al., 2004). Application of nifedipine (10 μM) reduced whole-cell I_{Ba} levels at all potentials, and the current density at 0 mV by 50% (Fig. 2Cb,d). Although nifedipine caused large reductions in the current amplitude at all potentials, it did not significantly affect current-voltage relationships (Fig. 2Cc). These results confirm that L-type Ca^{2+} channels are present on proliferating NPC membranes, and demonstrate that they are involved, at least in part, in the depolarization-induced effect on proliferation.

NMDA receptor activation induces extra VEGF secretion

Although NMDA and KCl were able to directly activate receptors and ion channels, it remained possible that they stimulated cell division by an indirect effect on the same or neighboring cells, causing them to release trophic factors involved in excitation-induced proliferation. To test this possibility we first determined whether excitation altered the expression of a number of releasable factors. Quantitative real-time (RT)-PCR analysis showed that, compared with untreated controls, the levels of brain-derived neurotrophic factor (BDNF), platelet-derived growth factor (PDGF) and vascular endothelial growth factor (VEGF) mRNAs was increased 72 hours (but not 24 hours) after the single 24-hour pulse of NMDA or KCl (Fig. 3A). The NMDA-induced expression of these factors was blocked by MK801. We tested whether VEGF, recently found to be active in neurogenesis (Cao et al., 2004; Shetty et al., 2005), was released from the NPCs into the culture medium where it could act as a paracrine and/or autocrine signal. A significant amount of VEGF appeared to be released into the medium in response to a single NMDA pulse (Fig. 3B), and application of MK801 30 minutes prior to the addition of NMDA completely blocked the release of VEGF. VEGF release was not detected upon NMDA stimulation for 72 hours, probably because of the reduced cell

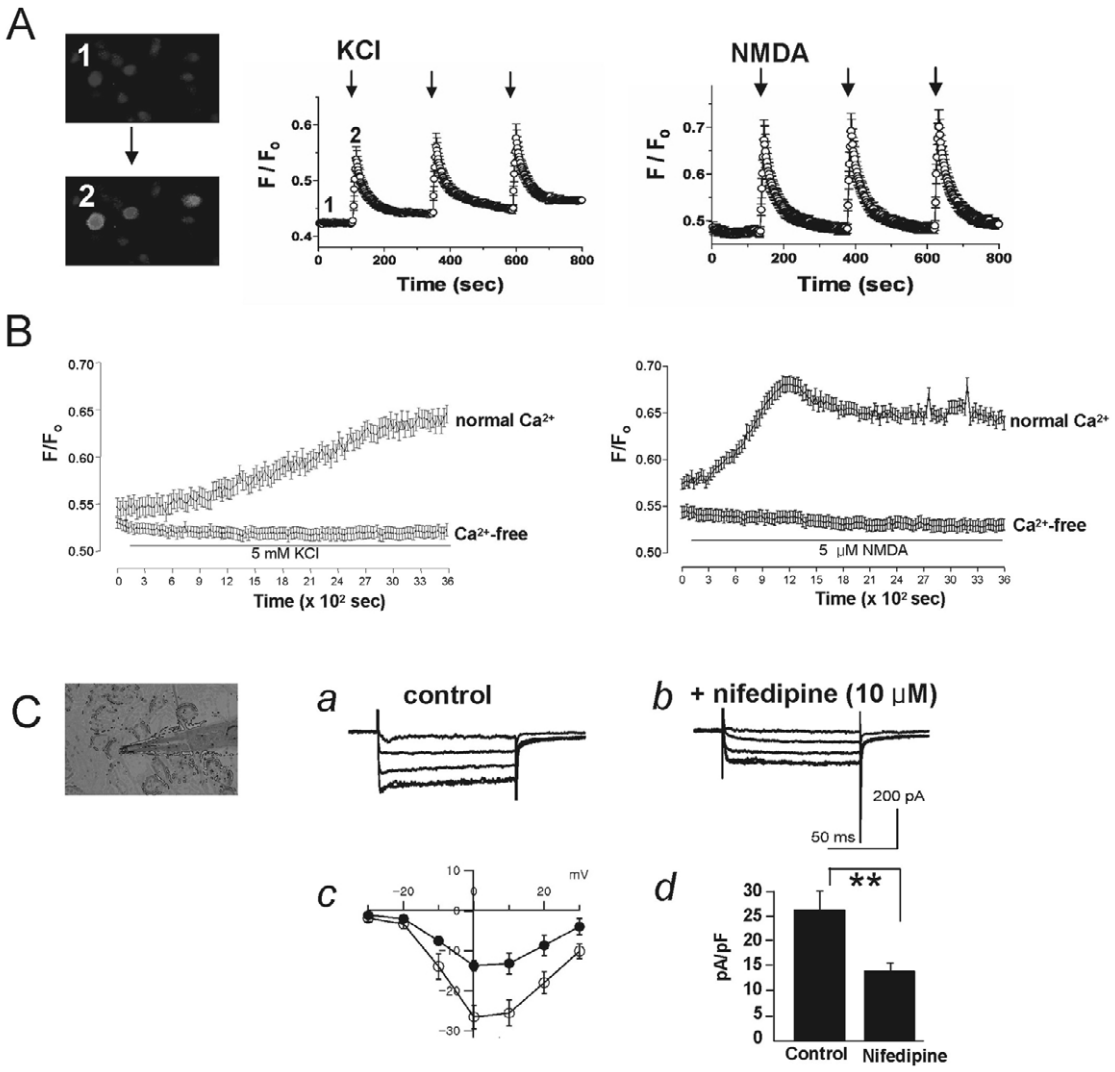

Fig. 2. Excitation-induced Ca^{2+} influx and expression of Ca^{2+} channels in proliferating NPCs. (A) Representative images from Ca^{2+} imaging. 1, Before drug treatment; 2, after drug treatment. Cells cultured for 3 DIV in the presence of bFGF were incubated with 5 μM fura-2/AM, then exposed to either 50 mM KCl (left graph) or 100 μM NMDA (right graph) for 10 seconds at the times indicated by arrows. The acetoxymethyl-ester form of fura-2 (fura-2/AM, Molecular probes, Eugene, OR) was used as the fluorescent Ca^{2+} indicator. Cells were incubated for 40-60 minutes at room temperature with 5 μM fura-2/AM and 0.001% Pluronic F-127 in a HEPES-buffered solution composed of 153 mM NaCl, 2 mM KCl, 1 mM $MgCl_2$, 2.5 mM $CaCl_2$, 10 mM HEPES, 10 mM glucose, pH adjusted to 7.4 with NaOH. The cells were then washed with HEPES-buffered solution and placed on an inverted microscope (Olympus, Japan). The 5 mM KCl-HEPES buffer contained: 150 mM NaCl, 5 mM KCl, 1 mM $MgCl_2$, 2.5 mM $CaCl_2$, 10 mM HEPES, 10 mM glucose, pH adjusted to 7.4 with NaOH. For experiments without extracellular Ca^{2+}, Ca^{2+} was not added to the external solution containing 2 mM EGTA. The cells were illuminated using a xenon arc lamp, and the required excitation wavelengths (340 and 380 nm) were selected by means of a computer-controlled filter wheel (Sutter Instruments, CA). Emitter fluorescence light was reflected through a 515 nm long-pass filter to a frame transfer cooled CCD camera, and the ratios of emitted fluorescence were calculated using a digital fluorescence analyzer. All imaging data were collected and analyzed using Universal Imaging software (West Chester, PA). Fura-2/AM fluorescence is expressed as F/F_0; increased fluorescence indicates elevated $[Ca^{2+}]_i$. Values of the mean ± s.e.m. of all the loaded cells are shown (n=52 for KCl; n=19 for NMDA). The images are of a field of cells at the time points corresponding to 1 and 2. (B) Continuous fluorometric $[Ca^{2+}]_i$ recording in proliferating NPCs loaded with fura-2/AM. Bath application of 5 mM KCl (left graph) or 5 μM NMDA (right graph) causes a time-dependent elevation in $[Ca^{2+}]_i$ when Ca^{2+}-containing buffer was used (KCl, n=50; NMDA, n=50). However, the KCl- or NMDA-induced Ca^{2+} influx was abolished when Ca^{2+}-free extracellular buffer was used (KCl, n=50; NMDA, n=50). Values of the ± s.e.m. of all observed cells are shown. (C) Ba^{2+} currents were recorded using a whole-cell patch clamp technique (see Materials and Methods). Cells cultured for 3 DIV in the presence of bFGF were incubated with NMDA (5 μM) before recordings. (a-d) Currents recorded in the (a) absence or (b) presence of the L-type Ca^{2+} channel blocker nifedipine (10 μM). Current traces induced by test pulses of –20, 0, 10, 20 and 30 mV are superimposed in the middle and right panels. The NPCs, of which an image is shown in the left panel, were subjected to depolarizing test pulses every 10 seconds (pulse duration of 100 mseconds) from a holding potential of −40 mV. The I–V relationships were obtained by plotting peak current amplitudes as a function of test potentials ranging from –30 to +30 mV (n=4, ○, control; ●, 10 μM nifedipine) (c). (d) Summary of the effect of nifedipine on the current density measured at 0 mV. Bath application of 10 μM nifedipine attenuated the I_{Ba} densities (control, 26.7±3.0 pA/pF; nifedipine, 13.9±2.0 pA/pF; n=4, $^{**}P$<0.01). Error bars indicate ± s.e.m.

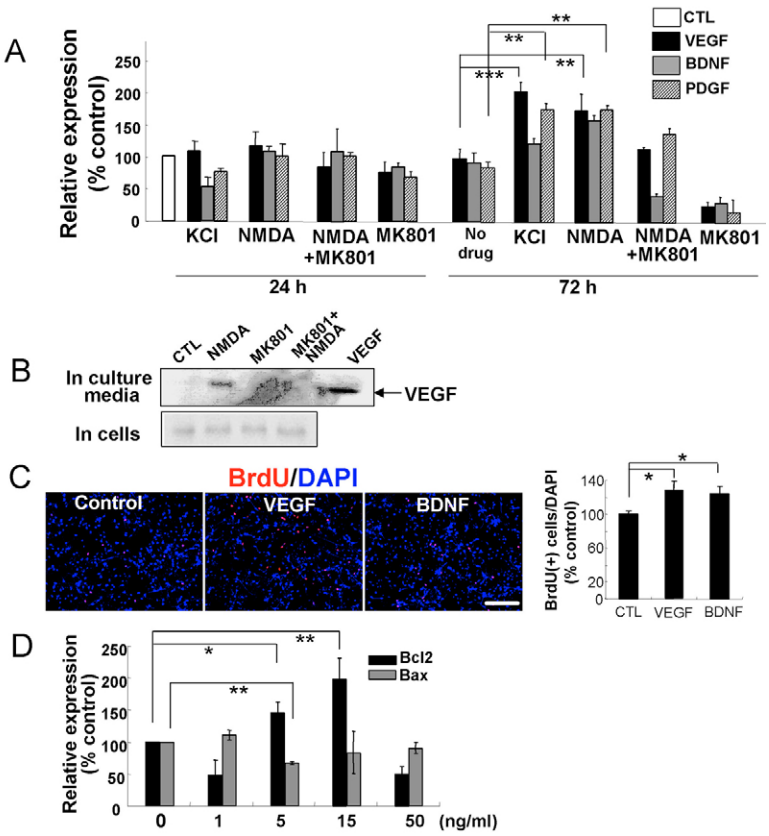

Fig. 3. NMDA stimulates the release of VEGF from proliferating hippocampal NPCs. (A) Real-time PCR analysis of BDNF, PDGF and VEGF mRNAs 24 hours and 72 hours after a single 24-hour pulse of each substance. The expression of each gene was normalized to the amount of GAPDH to obtain the relative level of its transcript (n=5 per group) and is shown relative to the expression levels in control cells at 24 hours. (B) Western blot of VEGF. Secretion of VEGF into the culture medium 72 hours after the single 24-hour pulse of each treatment. VEGF (10 ng/ml) was loaded as a positive control. (C) Addition of VEGF or BDNF increases the fraction of $BrdU^+$ (red). VEGF (50 ng/ml) or BDNF (50 ng/ml) was added to the culture medium in the absence of bFGF for 72 hours, and proliferating cells were labeled by BrdU for 1 hour before fixation. All the cells were counterstained with DAPI (blue). The percentage of $BrdU^+$ cells [BrdU(+)] cells is shown. Bar, 100 μm. (D) Quantitative RT-PCR analysis showing that Bcl2 and Bax mRNA levels were increased and decreased, respectively, after exogeneous VEGF application for 24 hours. Expression levels of Bcl2 and Bax were normalized to the amount of GAPDH expression to calculate the relative amount of gene transcript (n=3 per group). Expression levels at each concentration are depicted relative to the expression of the control 3 days after the onset of stimulation for comparison. MK, MK801. Error bars indicate ± s.e.m. CTL, control. *P<0.05, **P<0.01, **P<0.001.

number, as indicated in Fig. 1B. The amount of residual VEGF in cell extracts was the same in control and NMDA-stimulated cells. To see whether VEGF and BDNF promote proliferation we added them to cultures in the absence of bFGF, and counted the number of $BrdU^+$ cells. This number rose in a dose-dependent manner following VEGF or BDNF treatment, reaching a maximum increase of 122% and 119%, respectively, over the control value at a dose of 50 ng/ml (Fig. 3C) 72 hours after treatment. Therefore, it is likely that depolarization induces the release of endogeneous proliferation factors, including VEGF and BDNF; in turn, these factors appear to act as autocrine and/or paracrine signals for adjacent proliferating NPCs with a delay of at least 72 hours. Based on the recent study by Wada et al. (Wada et al., 2006), which demonstrated that VEGF-A signaling stimulates cell survival of definitive neural stem cells (d-NSCs), we investigated whether VEGF-A signaling increased the survival of hippocampal NPCs. Application of exogenous VEGF, mostly in a concentration of 5-15 ng/ml, increased the mRNA levels of the pro-survival factor Bcl2, whereas it decreased those of Bax, a proapoptotic factor (Fig. 3D). These results indicate that the depolarization-induced increase in the number of $BrdU^+$ cells are associated with enhanced cell survival.

NMDA-treated hippocampal NPCs undergo a G1-S-phase transition

We next examined whether NMDA-treated NPCs exhibit features consistent with a G1-S-phase transition using flow cytometric analysis of PI fluorescence. After 4 DIV in bFGF-containing medium, cells were present in all phases (G0-G1, S and G2-M phase) of the cell cycle, consistent with the heterogeneous nature of proliferating NPCs (Fig. 4A). The DNA content frequency histograms (Fig. 4A) revealed that, when proliferating NPCs were treated with a single pulse of NMDA for 24 hours and tested 72 hours after the stimulation, the proportion of G1-phase cells decreased (from 53% to 44%), and this was accompanied by an increase in the number of cells in S phase to approximately 10% from 5% in control cultures (Fig. 4A,B; P<0.05, respectively). Attempts to synchronize the cells with thymidine, a reversible inhibitor of mitosis (Merrill, 1998), were successful, because there was a marked decrease in the proportion of G1-phase cells (30%) and an increase in the proportion of S-phase cells (27%) (Fig. 4A,B). The effects of NMDA on cell cycle progression were blocked by MK801, and MK801 alone had no effect (Fig. 4A,B; P<0.001). Consistent with the data on BrdU incorporation, KCl slightly increased the proportion of S-phase cells (from 5% to 9%; Fig. 4B; P<0.05). These results provide further support for a role of excitation in increasing DNA synthesis in proliferating progenitors. The proportion of cells in G2-M increased by NMDA (Fig. 4B; CTL, 5.0±1.8; NMDA, 10.5±1.8, P<0.05), suggesting that NMDA receptor activation stimulated normal progression of the cells through G2-M phase to cell division.

To obtain insight into the mechanism by which NMDA facilitates cell cycle progression we examined the expression of retinoblastoma (Rb) protein, which is known to be involved in the G1-S-phase transition. Phosphorylated Rb (P-Rb, inactive) permits mitosis, while unphosphorylated (active) Rb inhibits it (Ferguson and Slack, 2001). The level of expression

of *P*-Rb^{Ser780} increased progressively over the 24-hour period after NMDA treatment (Fig. 4C), and there was a 50% reduction in the level of unphosphorylated Rb over the following 5 days (Fig. 4C). These observations suggest that proliferation instead of NPC differentiation may be induced by mild activation of NMDA receptors.

Our data thus demonstrate that, within 24 hours of excitation, primary proliferating NPCs from embryonic rats undergo several cellular and molecular changes that are not readily detectable until 72 hours after excitation. These changes include onset of DNA synthesis and production of proliferation factors. The delayed outcome suggests that cellular machinery needs to be translated in order for proliferation to increase.

NMDA receptor activation promotes delayed proliferation of hippocampal NPCs in vivo

To test whether NMDA receptor activation also stimulates proliferation of hippocampal NPCs in the intact brain, rats were injected intraperitoneally with NMDA and/or MK801, followed by immunohistochemical detection of BrdU in the subgranular zone (SGZ). A single systemic administration of NMDA reduced the number of BrdU$^+$ cells relative to controls when the animals were killed 3 days after administration (Fig. 5A,B). However, the number of BrdU$^+$ cells increased after a single injection of MK801. Administration of MK801 30 minutes prior to NMDA led to no change in proliferation. These results are consistent with previous findings (Nacher and McEwen, 2006). We next performed similar experiments

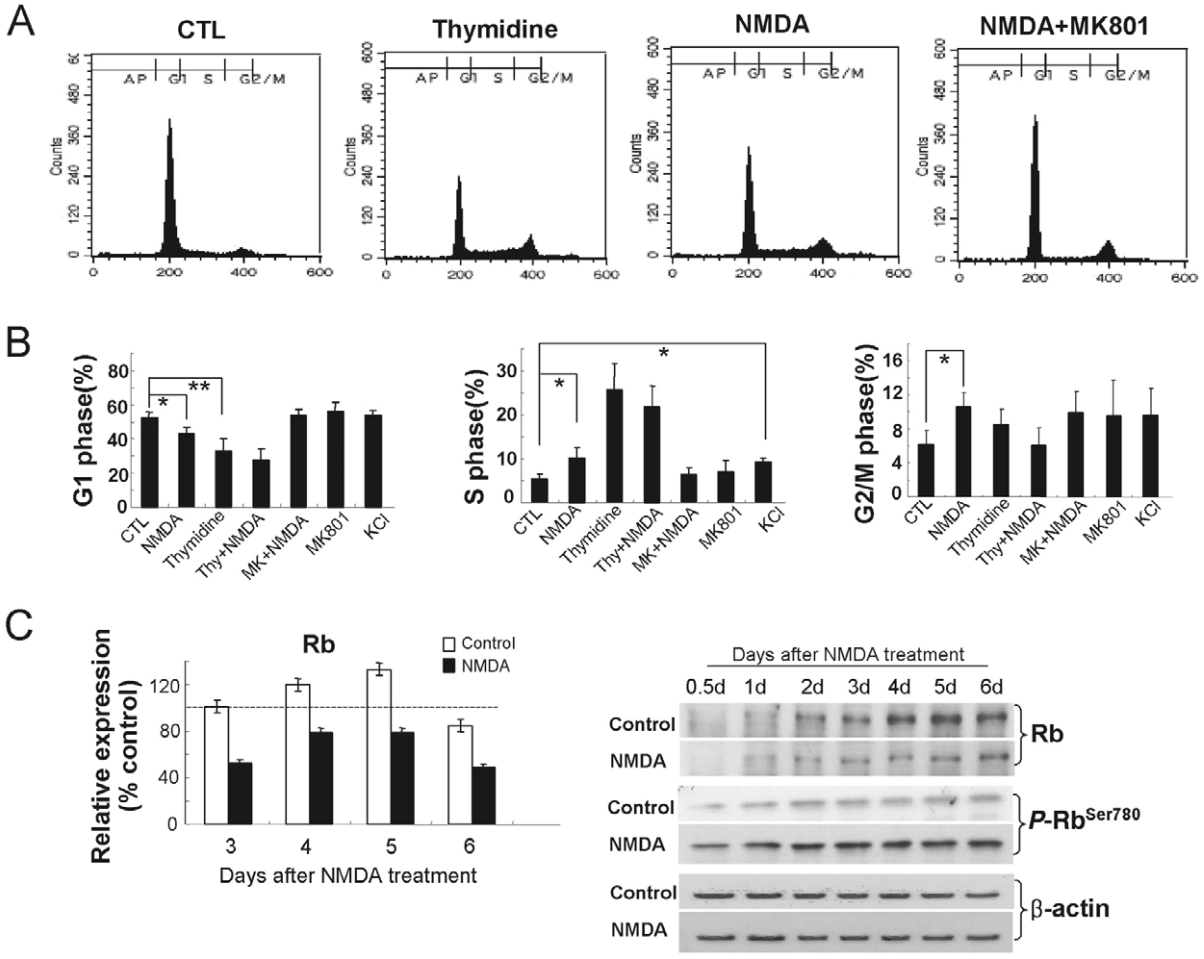

Fig. 4. NMDA modulates the cell cycle characteristics of cultured hippocampal NPCs. (A) Flow-cytometric histograms of DNA content as indicated by fluorescence intensity (FL-2 Area) on the *x*-axis and number of cells after staining with propidium iodide on the *y*-axis. Cells were incubated for 4 days with 20 ng/ml bFGF, with or without NMDA (5 μM), thymidine (3 μM), or MK801 (5 μM) for the first 24 hours. The results shown are from a single representative experiment. (B) Cells treated with various stimuli (as described in A) were analyzed for DNA content, and the areas under the peaks were compared. The numbers of cells with DNA contents corresponding to each cell cycle phase are expressed as percentages of the total sorted events. Values are the mean ± s.e.m. of 12 independent experiments. (C) A single-pulse treatment of NMDA decreases the level of Rb and increases that of *P*-Rb. Quantitative RT-PCR analysis (graph) showing that Rb mRNA levels were decreased by NMDA (5 μM) treatment for 24 hours. The expression of Rb was normalized to the amount of GAPDH to calculate the relative amount of the gene transcript (n=3 per group). Expression levels at each time point are depicted relative to the expression of the control 3 days after the onset of stimulation for comparison. Representative western blots showing that the level of *P*-Rb^{Ser780} was increased by NMDA for up to 6 days, even when NMDA stimulation was restricted to 24 hours (n=3). For comparison, blots were exposed for same duration in each antibody. AP, apoptosis; CTL, control; MK, MK801; Thy, thymidine; **P*<0.05, ***P*<0.01.

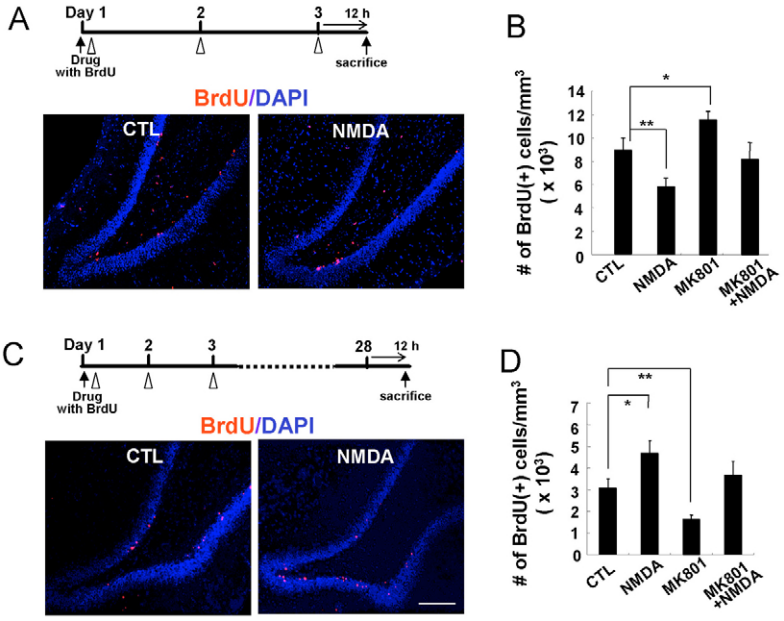

Fig. 5. Effect of a single systemic injection of NMDA on the number of BrdU$^+$ cells in the subgranular zone of the dentate gyrus 3 days and 28 days after administration. Diagrams show the way animals were treated (see Materials and Methods); arrows indicate drug application; arrowheads indicate BrdU detection. (A,B) Stereoscopic 3D-counting revealed that treatment with NMDA (100 mg/kg) decreased the number of BrdU$^+$ cells (red) when analyzed 3 days after treatment, whereas MK801 (50 mg/kg) increased it (saline, 8758±883 cells/mm^3; NMDA, 5720±510 cells/mm^3; MK801, 11,503±456 cells/mm^3, n=11 animals in each group). (C,D) Twenty-eight days after treatment, NMDA application resulted in an increase in the number of BrdU$^+$ cells, whereas MK801 produced a decrease (saline, 3048±417 cells/mm^3; NMDA, 4669±455 cells/mm^3, MK801, 1657±124 cells/mm^3, n=12 animals in each group). All cells were counterstained with DAPI (blue). Bar, 100 μm. Data are presented as the mean ± s.e.m. *P<0.05, **P<0.01.

except that the animals were killed 28 days after the single systemic injection. We found that the number of BrdU$^+$ cells was higher in the animals injected with NMDA and lower in those injected with MK801 compared with animals injected with saline as a control (Fig. 5C,D). The BrdU$^+$ cells both in NMDA- and MK801-injected animals were shown to express NeuroD (data not shown), which is functionally important both in differentiation and maturation of neurons (Kim et al., 2006). These results suggest that NMDA receptor activation increases the number of BrdU$^+$ NPCs in the intact hippocampus possibly via an increased survival similar to that observed in the in vitro model.

Stronger activation of NMDA receptors increases neuronal differentiation of NPCs

We next asked whether the same moderate excitation affects neuronal differentiation. To see whether the single pulse of NMDA (5 μM) stimulated neuronal differentiation of the NPCs, we induced differentiation of NPCs by withdrawing bFGF in the presence of NMDA for 24 hours, and examined the cells 72 hours after stimulation. Following this protocol we detected no change in the number or morphology of β-tubulin type III (Tuj1)-positive (Tuj1$^+$) cells (data not shown). However, NMDA (5 μM) treatment on 3 consecutive days did increase the density and number of Tuj1$^+$ neurons (Fig. 6A-C; P<0.001). However, MK801 (5 μM) addition prior to each NMDA treatment (Fig. 6B) blocked the increase in the number of Tuj1$^+$ cells, suggesting that NMDA receptor activation favors the acquisition of the neuronal phenotype. NMDA also caused an increase in the fraction of microtubule associated protein-2 (MAP2)-positive (MAP2$^+$) cells, suggesting that the maturation of postmitotic neurons was altered by NMDA receptor activation (Fig. 6D,E). The density of cells expressing the astroglial marker glial fibrillary acidic protein (GFAP), did not change upon NMDA treatment (Fig. 6E). Together, these data demonstrate that excitation promotes the acquisition and maturation of the neuronal phenotype.

Features of the axonal arborization in Tuj1$^+$ neurons formed in the presence of NMDA were readily recognized as different. We determined the number of axonal branch points, a frequently-used morphometric parameter, in the Tuj1$^+$ neurons. Although main axons exiting from the soma were evident in most of the Tuj1$^+$ neurons, cultures differentiated in the presence of NMDA contained neurons that had many more local axonal arborizations (>5 axonal branch points) than the neurons in control cultures, and this effect of NMDA was blocked by MK801 (Fig. 6F,G). In addition, the main axons of neurons formed in the presence of NMDA gave rise to daughter axon collaterals with much greater numbers of varicosities than those in the control cells (Fig. 6H). The differentiating cells also responded to NMDA and KCl by an increase of $[Ca^{2+}]_i$, as assessed by Ca^{2+} imaging (Fig. 6I), suggesting that Ca^{2+} is a key cytosolic factor in the NMDA-induced responses.

We also observed that NMDA treatment caused a marked increase in the expression of NMDA receptor subtype genes and α1D (the pore-forming subunit of L-type Ca^{2+} channels) in differentiating NPCs (Fig. 7). The increases in expression of the receptor subtype gene were more pronounced in differentiating NPCs than in proliferating NPCs.

NeuroD expression during NMDA-stimulated neuronal differentiation

To determine whether the observed changes in differentiation were related to the immediate proneural impact of NMDA receptor activation, we measured the expression of basic helix-loop-helix (bHLH) transcription factors. *NeuroD* is a downstream regulator of neuronal differentiation that controls the expression of genes required for terminal differentiation of dentate gyrus (DG) granule cells (Schwab et al., 2000). *NeuroD* mRNA expression was stimulated by NMDA (Fig. 8B), with a maximal effect when 5 μM was applied daily for 3 consecutive days. *Ngn1* is thought to positively regulate neuronal development at the level of postmitotic differentiation (Lee, 1997), and the homeodomain transcription factor *Emx2* plays a role in the developing hippocampus (Bishop et al., 2002). Both genes were strongly upregulated in the NMDA-

treated cells, (Fig. 8B) and their expression was blocked by MK801 (Fig. 8C). Quantitative mRNA analysis showed that the level of NeuroD mRNA was increased following NMDA treatment in a dose-dependent manner (Fig. 8D), and remained elevated by repetitive stimulation of NMDA for 72 hours, together with its translated form (Fig. 8E), as expected for a gene required for neuronal function. Since we were able to detect a secretion of VEGF from proliferating NPCs upon NMDA treatment, we further wanted to assess whether differentiated NPCs also respond to NMDA and release VEGF. To be able to relatively compare the amount of VEGF that might be secreted from astrocytes, the other major cell type in our differentiated cultures, astrocyte cultures were obtained and exposed to NMDA. In response to NMDA stimulation, differentiated NPCs released a significant amount of VEGF into the medium, and application of MK801 30 minutes prior to the NMDA application largely blocked the release of VEGF (Fig. 8F). It appeared that NMDA stimulation of astrocytes did not stimulate the secretion of VEGF at a detectable range. These results suggest that VEGF release upon NMDA application in our culture system was primarily accomplished by neurons but not astrocytes.

In order to investigate whether Ca^{2+} influx via VACC was capable of eliciting similar effects on gene expressions, KCl and BayK8644 were used. Depolarization by either KCl or BayK8644 also increased *NeuroD* mRNA expression (Fig. 8G), and the effect was more prominent by repetitive pulses over 72 hours than a single pulse for 24 hours. The effects of KCl and BayK8644 were inhibited by nifedipine, whereas nifedipine alone had little effect on the level of *NeuroD* mRNA. These results indicate that Ca^{2+} influx via L-type Ca^{2+} channels also mediates *NeuroD* expression leading to neuronal

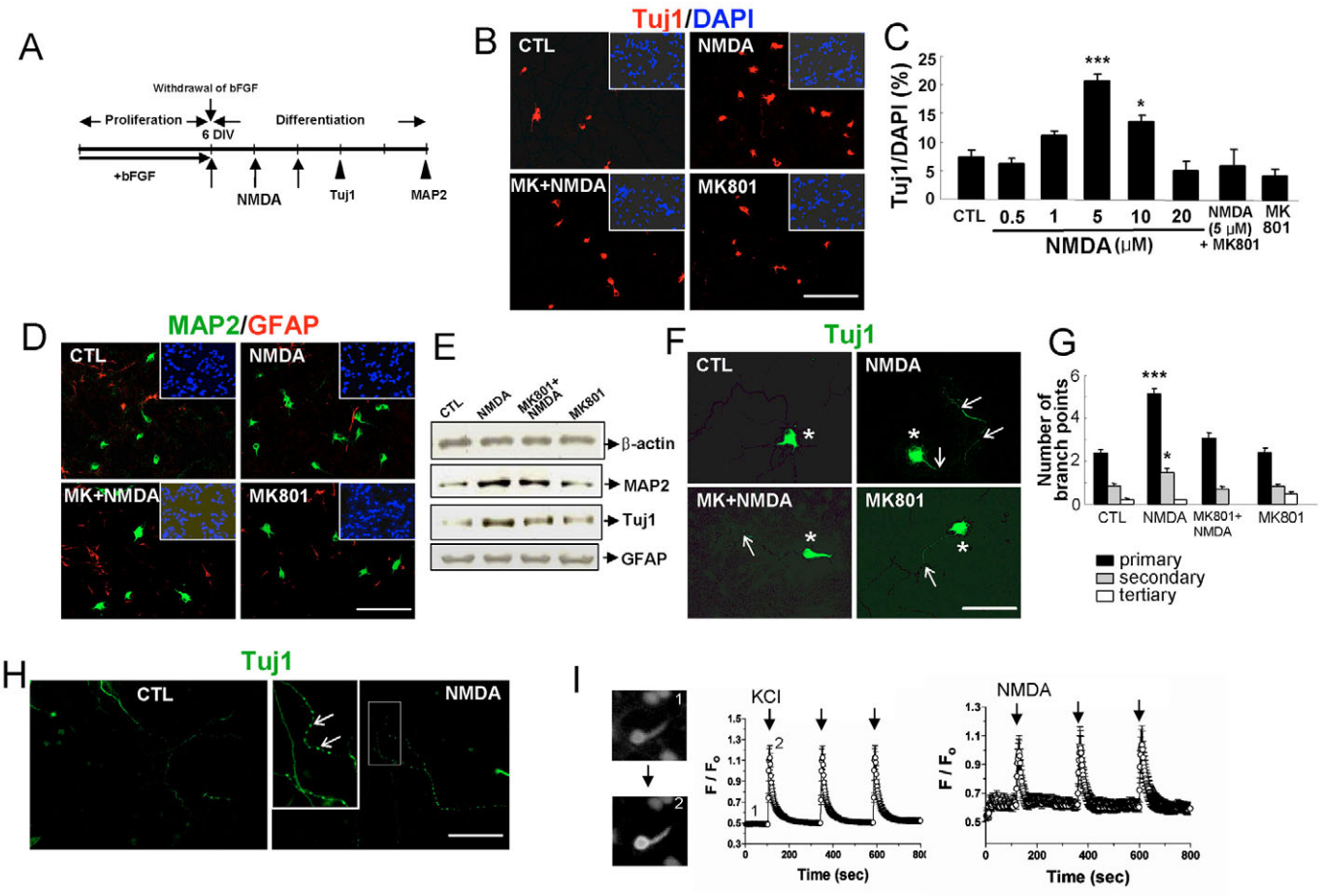

Fig. 6. Excitation increases acquisition of the neuronal phenotype and neuronal maturation of NPCs. Cells were induced to differentiate by withdrawal of bFGF in the presence of NMDA or MK801 for 3-5 days, followed by either dual immunocytochemistry or western blotting. (A) Diagram illustrating the experimental procedure. (B,C) Immunolabeling for Tuj1 (red). (B) $Tuj1^+$ cells were counted and numbers are expressed as the change in percentage compared with DAPI-positive cells in four experiments. (D) Dual-label immunocytochemistry for $MAP2^+$ (green) and $GFAP^+$ (red) cells 5 days after inducing differentiation. (E) Western blots showing that NMDA increased the expression of Tuj1 and MAP2 in differentiating NPCs and had little effect on the expression of the astroglial marker GFAP. (F) Immunocytochemical analysis showing that NMDA increased the number of neurons with axonal arborizations. Asterisks indicate soma; arrows indicate branch points. (G) The number of axons exiting the soma (1' axon) and axonal branches arborizing from 1' axons (2' axons) were counted in neurons immunostained for Tuj1 (n=100 cells per treatment). (H) Synaptic varicosities (arrows) were increased by NMDA treatment. Inset, enlargement of the field indicated by the box. (I) Representative images from Ca^{2+} imaging. Differentiated cells (8 DIV) were treated as described for Fig. 2A. The mean values of all loaded cells are shown (n=10 for KCl; n=16 for NMDA). Images show a field of cells at time points corresponding to 1 and 2. MK, MK801. *P<0.05, ***P<0.001. Bars, 50 μm (B,C), 20 μm (F), 5 μm (H).

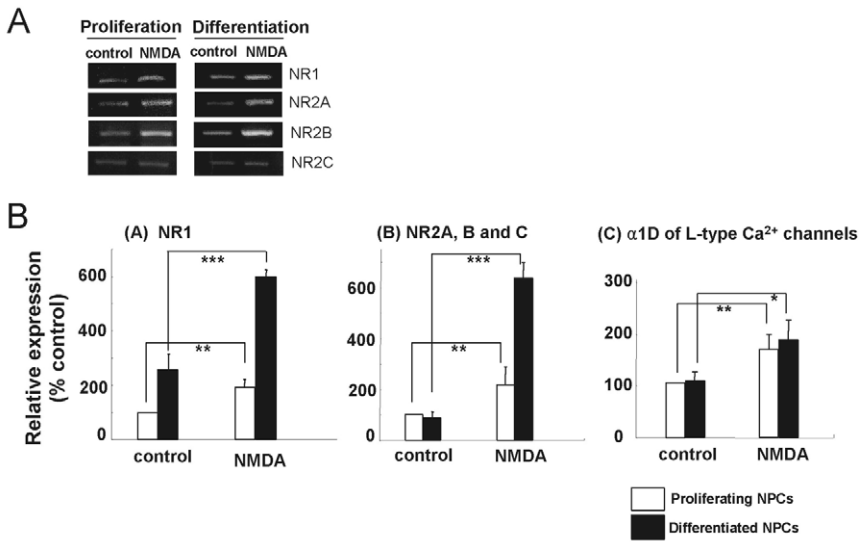

Fig. 7. NMDA receptor subunit gene expression during NMDA-induced proliferation and differentiation. Gene expression was investigated by semi-quantitative RT-PCR (A) and quantitative RT-PCR (B). Proliferating NPCs were treated with NMDA for 24 hours in the presence of bFGF and mRNA was extracted 72 hours after the stimulation. For differentiation, NPCs were treated daily with NMDA for 3 days in NB medium, and mRNA was isolated 24 hours after the last stimulation. The primer sets used for amplification of different subunits are listed in Materials and Methods. **P*<0.05, ***P*<0.01, ****P*<0.001.

differentiation. By contrast, the expression of *Id2* (a bHLH gene that inhibits development of the neuronal phenotype) was prominently downregulated by NMDA treatment for 72 hours (Fig. 8G). Excitation stimuli (such as KCl and BayK8644) also decreased *Id2* mRNA levels 72 hours after the stimuli, and nifedipine appeared to increase *Id2* expression within the first 24 hours of treatment. Together, these data demonstrate that Ca^{2+} influx following excitation of hippocampal progenitors induces gene expression patterns consistent with neuronal differentiation.

Discussion

Using a variety of approaches, we have demonstrated the neurogenic potential of mild excitation of embryonic hippocampal NPCs. Our results suggest that excitation primarily triggers mitosis via an increase in $[Ca^{2+}]_i$, potentially acting as a second messenger. However, our observations of high-density cell cultures do not exclude the possibility that depolarization-dependent release of mitogenic factors from the NPCs indirectly promotes the proliferation of NPC populations. Our electrophysiological data indicate that the I_{Ba} represents high-voltage-activated Ca^{2+} channel (HVA-CC) currents because the currents were activated at –20 mV and higher. These results are in good agreement with previous findings by Cai and co-workers and Sah and co-workers, demonstrating that primary rat embryonic NPCs in vitro expressed HVA-CC with similar electrophysiological features (Cai et al., 2004; Sah et al., 1997). Data from both Ca^{2+} imaging and whole-cell recording of L-type Ca^{2+} channels are consistent with the involvement of $[Ca^{2+}]_i$ and Ca^{2+} channel activation (including activation of L-type Ca^{2+} channels) in excitation-induced NPC proliferation. The fact that the effect of KCl on the number of $BrdU^+$ cells was blocked by nifedipine supports this possibility and indicates that the L-type of VACCs are activated by KCl in the NPCs. It is also likely that other VACCs, such as N-type, P/Q-type and R-type channels, are responsible for Ca^{2+} influx because nifedipine reduced the whole-cell I_{Ba} level by 50%. Furthermore, blockade of the NMDA-induced increase in the proportion of $BrdU^+$ and S-phase cells by the noncompetitive NMDA blocker MK801 is consistent with a role of Ca^{2+} influx in proliferation of the NPCs. Presumably, when we induced mild depolarization (5 mM KCl) or NMDA receptor activation (5 μM NMDA) for a prolonged period (24 hours), a persistent low level of membrane depolarization resulted in an increase in $[Ca^{2+}]_i$ that may not have been as high as that induced by 20 mM KCl or 50-300 μM glutamate in previous studies (Deisseroth et al., 2004; Wada et al., 2006). Ca^{2+} imaging with continuous application of 5 mM KCl or 5 uM NMDA demonstrated this was the case. Recently, it has been proven that the voltage-independent transient receptor potential cation channel, subfamily C, member 1 (TRPC1) plays a role in NPC proliferation by contributing to the bFGF-induced Ca^{2+} influx (Fiorio Pla et al., 2005). Thus, it is likely that other members of Ca^{2+} channels expressed by NPCs in addition to VACCS mediate the Ca^{2+} influx required for the self-renewal of proliferating NPCs.

It is generally believed that Ca^{2+} plays an important regulatory role in neural cell proliferation (Rosen and Greenberg, 1996). The work done by Haydar et al. (Haydar et al., 2000) demonstrated that glutamate (50 μM) and GABA (30 μM) increase proliferation in the ventricular zones, whereas they decrease DNA synthesis in the SVZ. However, a recent study demonstrated that Ca^{2+} influx due to excitation did not affect the proliferation of adult hippocampal NPCs (Deisseroth et al., 2004). Moreover, a pioneering study by LoTurco et al. (LoTurco et al., 1995) demonstrated that both KCl (20 mM) and glutamate (100 μM) depolarized embryonic cortical NPCs and inhibited DNA synthesis. $GABA_A$-receptor-mediated depolarization in neural stem cells of the adult SVZ inhibited their proliferation (Kriegstein, 2005). Generally, appearance of intracellular Ca^{2+} due to NMDA receptor activation seemed to decrease proliferation (Nacher and McEwen, 2006). The discrepancy between these studies and ours could be owing to two major differences: the excitation paradigm and the origins of the NPCs. In contrast to mild excitation over a period of 24 hours, as used in our present study, the adult hippocampal NPCs and embryonic cortical NPCs were exposed briefly (5 minutes) to 20 mM KCl, 50 μM glutamate or 50 μM NMDA. It thus appears that Ca^{2+} and depolarization can have both positive and negative effects on cell proliferation depending on the level of excitation, the origins and developmental stage of NPCs.

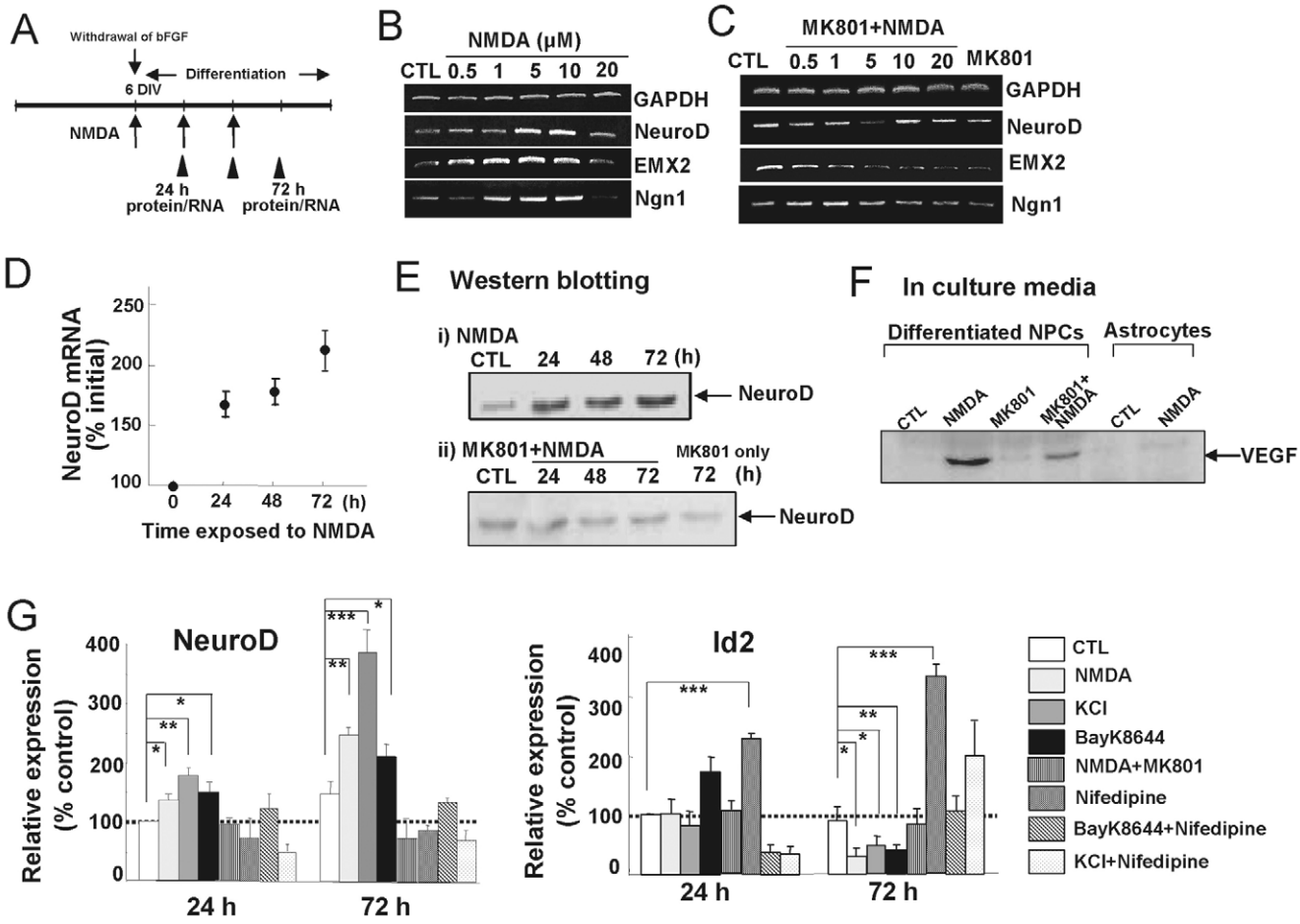

Fig. 8. NMDA regulates the activity of proneural bHLH, homeogene transcription factors and VEGF secretion in differentiated NPCs. (A) Diagram illustrating the experimental procedure. (B) Semiquantitative mRNA analysis of the transcription factors *NeuroD*, *Ngn1* and *Emx2*. (C) Expression of *NeuroD*, *Ngn1* and *Emx2* was blocked by MK801. Cells were treated daily for 3 consecutive days and analyzed 24 hours after the last stimulation in B,C. (D) RT-PCR analysis of *NeuroD*. Excitation with NMDA (5 μM) in medium permissive of neuronal differentiation caused an increase in the expression of *NeuroD* as NMDA treatment was repetitive at an interval of 24 hours. (E) Western blot analysis of *NeuroD* in the presence of NMDA, and in the presence or absence of MK801. Cells were treated with a pulse of NMDA for 24 hours, two pulses over 48 hours or three pulses over 72 hours and analyzed 24 hours after the stimulation in D-E. (F) Western blot analysis of secretion of VEGF into the culture medium from the differentiated NPCs and astrocytes after the three pulses of each treatment over 72 hours. (G) Real-time PCR analysis of *NeuroD* and *Id2* following various stimuli. Cells were daily treated with each stimulus at a single pulse for 24 hours or three pulses over 72 hours and analyzed 24 hours after the last stimulation. Values are the mean ± s.e.m. (n=5). Gene expression levels are depicted relative to the expression of GAPDH, and calculated relative to expression in control differentiating cells, which have been allowed to differentiate for corresponding periods of time. *P<0.05, **P<0.01, ***P<0.001.

A second explanation for the increase in the number of proliferating cells could be the release of mitogenic and survival factors following excitation. This possibility is supported by our observation that the proliferating NPCs grown in NMDA-containing medium produced and secreted VEGF, and VEGF has been shown to be mitogenic (Shetty et al., 2005). We also observed that the level of VEGF in the culture medium was higher 72 hours after the beginning of the excitation than after 24 hours (see Figs 1 and 4). These results, combined with the observation that the proportion of $BrdU^+$ and S-phase cells increased 72 hours after the onset of stimulation, led us to conclude that delayed responses, such as the synthesis and release of mitogenic factors, contribute to the proliferation induced by mild excitation in addition to immediate responses such as the opening of ion channels. Moreover, the mitogenic factor might act as a survival factor. In support of this, we found upregulated expressions of Bcl2 and donwregulated expressions of Bax following application of exogeneous VEGF. It is noticeable that VEGF is released from differentiated NPCs only upon NMDA application (Fig. 8F). Therefore, NMDA receptor stimulation might also be involved in the differentiation of NPCs by mediating the release of trophic factors. Very recently it has been shown that NMDA receptor activation competitively regulates the selective survival of new neurons and, thereby, the formation of neural circuits (Tashiro et al., 2006). The pro-survival effects of NMDA receptor activation on new cells may well explain our results from the in vivo experiments showing that NMDA receptor activation resulted in an increase in the number of $BrdU^+$ cells 28 days, but not 3 days, after NMDA

administration. Future work using a combination of excitation and addition of cytokines should shed light on the intracellular signaling pathways promoting the proliferation, and probably the survival, of NPCs.

Previous studies have shown that NPC cultures derived from E18 rat hippocampus appeared to be composed of multiple distinct cell types (Limke et al., 2003). Therefore, we assessed the fraction of NPCs versus neuronal/glial progenitor populations in our culture system. In doing so, we wanted to demonstrate that the observed effects on proliferation and VEGF secretion upon NMDA treatment are due to the activation of NPCs instead of neuronal progenitors. Characterization of our passaged proliferating cells revealed that ~87% of the cells expressed *Lex* (supplementary material Fig. S2), a stem cell marker (Ganat et al., 2006), suggesting that the majority of our cells are indeed stem cells as previously characterized (Kim et al., 2004). To further assess the contribution of neuronal or glial progenitors to our cell culture system, cells were examined for the expression of doublecortin (DCX), the polysialylated form of the neural cell adhesion molecule (PSA-NCAM; both markers for neuronal progenitors) or A2B5 (a marker for glial progenitors). PSA-NCAM and DCX were evident in only ~0.3-0.5% and ~1.3-1.7% of all cells, respectively, and A2B5 expression was found in ~1-2% of all cells. These results indicate that there is only a very small subpopulation of neuronal or glial progenitors in our culture system. Therefore, a possible contribution of neuronal progenitors to the observed effects upon NMDA treatment in our cell culture seems negligible. Taken together, these results led us to suggest that NMDA might be directly acting on NPCs and, in turn, indirectly acting on neighboring NPCs via the release of survival and/or mitogenic factors such as VEGF.

In addition to our observations on the proliferation of NPCs we found that excitation promoted the neuronal differentiation of NPCs, accompanied by rapid induction of proneural genes, and that this occurred primarily via Ca^{2+}-dependent pathways. Although we could not determine whether diffusible factors were being generated by the differentiating neurons because our in vitro assay system contained both neurons and astroglial cells, we believe that excitation is likely to induce the secretion of growth factors from the neurons differentiated from NPCs in vitro, and that this results in the activation of neurogenic processes based on our results that differentiated NPCs but not astrocytes release VEGF following excitation with NMDA. Moreover, we observed that NMDA (5 μM) did not induce cell death of astrocytes (data now shown), indicating that the effects of NMDA on neuronal differentiation are not indirectly highlighted through selective cell death of non-neuronal cells. Taken together, these results imply that NMDA acts mainly on differentiated neurons in our assay system.

Our results raise the question of how NMDA receptor activity can promote both proliferation and differentiation during neurogenesis. Our results suggest that a higher level of intracellular Ca^{2+} is required to stimulate differentiation than is needed to promote cell division. The differential Ca^{2+} responsiveness might be related to the capability of proliferating and differentiating cells to sequester intracellular Ca^{2+}. Hence, the level of glutamate, which changes in response to activity, may be a key factor determining whether NPCs proliferate or differentiate. In this way, a single parameter (intracellular Ca^{2+}) may control the different responses of NPCs needed for neurogenesis. Since NPC populations in vivo are heterogeneous with respect to developmental stage (proliferation versus differentiation), different levels of excitation may control their choice between proliferation and differentiation. In addition, the link between NMDA receptor activation and altered neurogenesis in vivo may be both direct and indirect as in our in vitro study. We conclude that activation of the NMDA receptor may play a role in proliferation of particular populations of NPCs. This role does not solely involve a direct effect on the NMDA receptors of the NPCs whose proliferation is stimulated, but release of mitogenic and/or survival factors may also be implicated. Furthermore, NMDA receptor activation may elicit both multiplication and differentiation, depending upon the NPC population under consideration.

Materials and Methods

Hippocampal NPC cell culture

Pregnant adult Sprague Dawley rats (Harlan Sprague Dawley, Indianapolis, IN) were used, following the procedures described by Kim et al. (Kim et al., 2004). Briefly, hippocampi were dissected from embryonic day 16.5 (E16.5) rat embryos into HBSS without Ca^{2+} or Mg^{2+}. Cells were plated on 10-cm dishes coated with 15 μg/ml poly-L-ornithine and 1 μg/ml fibronectin (Invitrogen, Carlsbad, CA) at 2.5×10^4 cells/cm^2 in N2 medium and incubated at 37°C in 95% air 5% CO_2 atmosphere. N2 medium was composed of DMEM-F12 supplemented with 100 U/ml penicillin-streptomycin, 8.6 mM glucose, 20 mM sodium bicarbonate, 2 μM progestanin, 3 μM sodium selenite, 0.1 mM putrescine, 25 μg/ml insulin and 100 μg/ml apo-transferrin. For experiments with inhibitors, MK801 (5 μM; TOCRIS, Northpoint, Avonmouth, UK), 6-cyano-7-nitroquinoxaline-2,3-dione (CNQX, 10 μM) or nifedipine (3 μM) (both Sigma, St Louis, MO) in dimethyl sulfoxide (DMSO, 0.01%) was added to cells 30 minutes before the addition of NMDA or BayK8644 (3 μM, Sigma). VEGF165 (R&D Systems) was dissolved in phosphate-buffered saline (pH 7.4). Control cultures were treated with an equivalent concentration of DMSO.

Basic fibroblast growth factor (bFGF, 20 ng/ml, R&D Systems, Minneapolis, MN) was added daily to expand the population of NPCs. For high-density cultures, cells at 80% confluence were passaged once in 24-well plates on the fourth day in vitro (4 DIV); the cells were then expanded up to 10 DIV in the absence or presence of NMDA (1-20 μM) or AMPA (5 μM). Upon reaching 5-6 DIV, the expanded cells were allowed to differentiate for up to 5 days in the absence of bFGF with or without NMDA (5 μM) in neurobasal (NB) medium. For various chemical stimulations cells were treated as indicated above. Acetone precipitation was used to concentrate culture media (Bollag and Edelstein, 1991). For astrocytic cultures, hippocampal NPCs at 80% confluence were passaged once on 4 DIV and cells were grown in N2 medium supplemented with 2% (v/v) fetal bovine serum (FBS). After 2-3 days, the subconfluent cultures were passaged again and cultured in N2 medium supplemented with 10% FBS for 3 days. These cultures revealed that at least 95% of the cells were positive for the astrocyte-specific marker GFAP.

Assays of BrdU incorporation and cell death

BrdU (10 μM; Sigma, St Louis, MO) was added to cultures for 1 hour and the cells were then fixed. For the apoptosis assay we employed the terminal deoxynucleotidyl-transferase-mediated deoxyuridine triphosphate (dUTP) nick-end-labeling (TUNEL) assay using an in situ cell death detection POD kit (Roche Molecular Biochemicals, Basel, Switzerland). Cells were mounted in mounting medium using Vectashield® with 4', 6 diamidino-2-phenylindole (DAPI) (Vector Laboratories, Burlingame, CA).

Immunocytochemistry and western blot analysis

Cells were fixed with 4% paraformaldehyde/0.15% picric acid in PBS for 20 minutes. After exposure to antibodies, the cells were incubated in PBS containing Cy3-labeled (1:100; Jackson ImmunoResearch, West Grove, PA) or FITC-labeled (1:500; Molecular Probes, Eugene, OR) secondary antibodies, mounted in Vectashield® mounting medium for fluorescence analysis and photographed with a fluorescence microscope (Nikon, Tokyo, Japan). For western blot analysis, cells were prepared as previously described (Kim et al., 2004).

The following primary antibodies were used for immunocytochemistry: monoclonal β-tubulin type III (Tuj1) (Covance, Berkeley, CA; 1:500), monoclonal MAP2 (Sigma-Aldrich; 1:200), monoclonal GFAP (ICN Biochemicals, Costa Mesa, CA; 1:100), polyclonal GFAP (Dako, Glostrup,

Denmark; 1:400), and BrdU (Accurate Chemical, Westbury, NY; 1:100). Antibodies used for western blotts were polyclonal NeuroD (Chemicon, Temecula, CA; 1:1000), monoclonal GFAP (ICN Biochemicals Ins; 1:600), polyclonal VEGF (R&D, Minneapolis, MN; 1:1000), polyclonal Rb (Santa Cruz, Delaware, CA; 1:800), or polyclonal *P*-Rb (Ser780) (Cell Signaling, Danvers, MA; 1:800) antibodies.

Real-time RT-PCR and quantitation of gene expression

Total RNA was prepared as described previously (Kim et al., 2004). Primers employed were: BDNF sense, 5′-GTGACAGTATTAGCGAGTGGG-3′, antisense, 5′-GGGTAGTTCGGCATTGC-3′; PDGF sense, 5′-TGCCTCTCTGCTGCTAC-CTG-3′, antisense, 5′-GTCGAAGGCGACCGGCCTGC-3′; VEGF, sense, 5′-AGGCTGCACCCACGACAGAAG-3′, antisense, 5′-TCACCGCCTTGGCTTGT-CAC-3′; Bcl2 sense, CTG TAC GGC CCC AGC ATG CG, antisense, GCT TTG TTT CAT GGT ACA TC; Bax sense, GGATGCGTCCACCAAGAAGC, antisense, CACCCTGGTCTTGGATCCAG; NeuroD sense, 5′-CTCAGTTCTCAGGACGA-GGA-3′, antisense, 5′-TAGTTCTTGGCCAAGCGCAG-3′; Id2 sense, 5′-TGAA-CGTTCTGCTCTACGACA-3′, antisense, 5′-AGAGGCATTCCCACTTCTCTA-3′; GFAP sense, 5′-GCAGACCTCACAGACGTTGCT-3′ antisense, 5′-AGGCTGG-TTTCTCGGATCTGG-3′; Rb sense, 5′-TCATGGAATCCCTTGCATGGC-3′ antisense, 5′-TGGCTTCTGAGTATGGAAGGC-3′; NR-1 sense, 5′-CTTGTCTG-AGGGGTTTCTGAG-3′, antisense, 5′-ACACAGGAGCGGGTAAAC-3′; NR2A-sense, 5′-GCGCGCAGCACGCCCCATTGCATC-3′; NR2A-antisense, 5′-GGGCCACAGCCTCCTGGTCCGTGTCA-3′; NR2B-sense, 5′-CCCAGCATC-GGCATCGCTGTGATCCTC-3′, antisense, 5′-CATGATGTTGAGCATGACGGA-AGCTTG-3′; NR2C sense, 5′-CTGGACCTGCCTCTGGAGATCCAGCCA-3′, antisense, 5′-GCGGTCCGCGACGGCGCGCACGCC-3′; NR-2A,B,C sense, 5′-GGGGTTCTGCATCGACATCC-3′, antisense, 5′-GACAGCAAAGAAGGCC-CACAC-3′; α1D sense, 5′-GCCGGATCCATCGTCACCTTCCAGGAGCA-3′, antisense, 5′-ATGGAATTCGCCACGAAGAGGTTGATGAT-3′. Primers for GAPDH, β-tubulin type III, Ngn1, and Emx2 have been described (Kim et al., 2006). The expression of each gene was normalized to the amount of GAPDH in order to calculate relative levels of transcript. Normalized expression values were averaged and average fold changes calculated. Student's *t*-test was used to determine statistical significance of differences.

Flow-cytometry analysis

Proliferating NPCs were analyzed with an Epics XL flow cytometer (Coulter, Fullerton, CA). Dissociated NPCs were fixed overnight in 70% ethanol-PBS, resuspended in PBS and treated with 25 μg/ml ribonuclease A (Sigma) for 1 hour at room temperature, followed by staining with 50 μg/ml propidium iodide (PI; Sigma). Argon-ion laser excitation (488 nm) was used to measure PI fluorescence with a 620 nm band-pass filter.

Patch-clamp recording

Whole-cell Ba^{2+} currents were recorded with an EPC8 amplifier (HEKA, Lambrecht, Germany). Filtered signals (10 KHz) from the amplifier were fed into an AD/DA converter (PCI-MIO-16E-4, National Instrument, Austin, TX), digitized at 20 kHz, and stored in a computer. Patch electrodes were fabricated from borosilicate glass capillaries (Hilgenberg, Malsfeld, Germany). The compositions of the external solution and internal pipette solution were as follows. The electrodes had resistances of 2.5-3.5 MΩ after filling with the internal solution described below. All experiments were performed at room temperature (20-24°C). The external solution contained (in mM): 130 NaCl, 5.4 KCl, 5 HEPES, 0.5 $MgCl_2$, 0.5 NaH_2PO_4, 10 $BaCl_2$, and 10 glucose (pH 7.4). Tetrodotoxin (TTX, 500 nM) was added to block Na^+ currents. The internal pipette solution contained (in mM): 90 Cs-gluconate, 20 CsCl, 2 $MgCl_2$, 5 Mg-ATP, 10 HEPES, 2.5 Na_2-creatine phosphate, 10 tetraethyl-ammonium chloride, and 10 ethylene glycol-bis-(β-aminoethyl ether)-*N*,*N*,*N*′,*N*′-tetra-acetic acid (pH 7.3).

Capacitative transients were compensated online, using the built-in compensation circuit. Current density (pA/pF) was calculated from measurements of current amplitudes (pA), and cell capacitance (pF) was read by adjusting the C_{slow} compensation knob on the amplifier. Data were analyzed with Clampfit software (Axon instruments, Foster City, CA) and are presented using Prism software (GraphPad, San Diego, CA).

In vivo drug injection and immunohistochemistry for BrdU

Adult male Sprague Dawley rats (2-months old) housed in a 12-hour light-dark cycle animal facility received a single injection of NMDA (100 mg/kg) or the non-competitive NMDA receptor antagonist MK801 (5 mg/kg) intraperitoneally in 0.9% saline. To measure cell proliferation, animals were injected intraperitoneally with BrdU dissolved in saline at 50 mg/kg every 12 hours for 3 days. When used, MK801 was injected into animals 30 minutes before the administration of NMDA. Animals were killed under pentobarbital anesthesia 12 hours after the last administration of BrdU, 3 days after the start of the NMDA and BrdU treatments. For rats killed 28 days after treatment, BrdU was injected daily in a similar way for the first 3 days. Rats were processed and BrdU was analyzed histochemically as described (Son et al., 2003). $BrdU^+$ cells were counted in the subgranular zone (SGZ).

This research was supported by a grant (M103KV010008-06K2201-00810) from the Brain Research Center (BRC) of the 21st Century Frontier Research Program funded by the Ministry of Science and Technology (Republic of Korea) awarded to H.S.

References

Arvidsson, A., Kokaia, Z. and Lindvall, O. (2001). *N*-methyl-*D*-aspartate receptor-mediated increase of neurogenesis in adult rat dentate gyrus following stroke. *Eur. J. Neurosci.* **14**, 10-18.

Bishop, K. M., Rubenstein, J. L. and O'Leary, D. D. (2002). Distinct actions of Emx1, Emx2, and Pax6 in regulating the specification of areas in the developing neocortex. *J. Neurosci.* **22**, 7627-7638.

Bollag, D. M. and Edelstein, S. J. (1991). *Protein Methods* (1st edn). New York: Wiley-Liss.

Cai, J., Cheng, A., Luo, Y., Lu, C., Mattson, M. P., Rao, M. S. and Furukawa, K. (2004). Membrane properties of rat embryonic multipotent neural stem cells. *J. Neurochem.* **88**, 212-226.

Cameron, H. A., McEwen, B. S. and Gould, E. (1995). Regulation of adult neurogenesis by excitatory input and NMDA receptor activation in the dentate gyrus. *J. Neurosci.* **15**, 4687-4692.

Cameron, H. A., Hazel, T. G. and McKay, R. D. (1998). Regulation of neurogenesis by growth factors and neurotransmitters. *J. Neurobiol.* **36**, 287-306.

Cao, L., Jiao, X., Zuzga, D. S., Liu, Y., Fong, D. M., Young, D. and During, M. J. (2004). VEGF links hippocampal activity with neurogenesis, learning and memory. *Nat. Genet.* **36**, 827-835.

Deisseroth, K., Singla, S., Toda, H., Monje, M., Palmer, T. D. and Malenka, R. C. (2004). Excitation-neurogenesis coupling in adult neural stem/progenitor cells. *Neuron* **42**, 535-552.

Ferguson, K. L. and Slack, R. S. (2001). The Rb pathway in neurogenesis. *Neuroreport* **12**, A55-A62.

Fiorio Pla, A., Maric, D., Brazer, S. C., Giacobini, P., Liu, X., Chang, Y. H., Ambudkar, I. S. and Barker, J. L. (2005). Canonical transient receptor potential1 plays a role in basic fibroblast growth factor (bFGF)/FGF receptor-1-induced Ca^{2+} entry and embryonic rat neural stem cell proliferation. *J. Neurosci*. **25**, 2687-2701.

Ganat, Y. M., Silbereis, J., Cave, C., Ngu, H., Anderson, G. M., Ohkubo, Y., Ment, L. R. and Vaccarino, F. M. (2006). Early postnatal astroglial cells produce multilineage precursors and neural stem cells in vivo. *J. Neurosci*. **26**, 8609-8621.

Haydar, T. F., Wang, F., Schwartz, M. L. and Rakic, P. (2000). Differential modulation of proliferation in the neocortical ventricular and subventricular zones. *J. Neurosci.* **20**, 5764-5774.

Kim, J. S., Chang, M. Y., Yu, I. T., Kim, J. H., Lee, S. H., Lee, Y. S. and Son, H. (2004). Lithium selectively increases neuronal differentiation of hippocampal neural progenitor cells both in vitro and in vivo. *J. Neurochem.* **89**, 324-336.

Kim, J. H., Lee, J.-A., Song, Y. M., Park, C. H., Hwang, S. J., Kim, Y. S., Kaang, B. K. and Son, H. (2006). Overexpression of calbindin-D_{28K} in hippocampal progenitor cells increases neuronal differentiation and neurite outgrowth. *FASEB J.* **20**, 109-111.

Kriegstein, A. R. (2005). GABA puts the brake on stem cells. *Nat. Neurosci*. **8**, 1132-1133.

Lee, J. E. (1997). Basic helix-loop-helix genes in neural development. *Curr. Opin. Neurobiol.* **7**, 13-20.

Levitt, P., Harvey, J. A., Friedman, E., Simansky, K. and Murphy, E. H. (1997). New evidence for neurotransmitter influences on brain development. *Trends Neurosci.* **20**, 269-274.

Limke, T. L., Cai, J., Miura, T., Rao, M. S. and Mattson, M. P. (2003). Distinguishing features of progenitor cells in the late embryonic and adult hippocampus. *Dev. Neurosci.* **25**, 257-272.

LoTurco, J. J., Owens, D. F., Heath, M. J., Davis, M. B. and Kriegstein, A. R. (1995). GABA and glutamate depolarize cortical progenitor cells and inhibit DNA synthesis. *Neuron* **15**, 1287-1298.

Luk, K. C., Kennedy, T. E. and Sadikot, A. F. (2003). Glutamate promotes proliferation of striatal neuronal progenitors by an NMDA receptor-mediated mechanism. *J. Neurosci.* **23**, 2239-2250.

Merrill, G. F. (1998). Cell synchronization. *Methods Cell Biol.* **57**, 229-249.

Nacher, J. and McEwen, B. S. (2006). The role of N-methyl-D-asparate receptors in neurogenesis. *Hippocampus* **16**, 267-270.

Rakic, P. and Komuro, H. (1995). The role of receptor/channel activity in neuronal cell migration. *J. Neurobiol*. **26**, 299-315.

Rosen, L. B. and Greenberg, M. E. (1996). Stimulation of growth factor receptor signal transduction by activation of voltage-sensitive calcium channels. *Proc. Natl. Acad. Sci. USA* **93**, 1113-1118.

Sah, D. W. Y., Ray, J. and Gage, F. H. (1997). Regulation of voltage- and ligand-gated currents in rat hippocampal progenitor cells in vitro. *J. Neurobiol*. **32**, 95-110.

Schwab, M. H., Bartholomae, A., Heimrich, B., Feldmeyer, D., Druffel-Augustin, S., Goebbels, S., Naya, F. J., Zhao, S., Frotscher, M., Tsai, M. J. et al. (2000). Neuronal basic helix-loop-helix proteins (NEX and BETA2/NeuroD) regulate terminal granule cell differentiation in the hippocampus. *J. Neurosci*. **20**, 3714-3724.

Shetty, A. K., Hattiangady, B. and Shetty, G. A. (2005). Stem/progenitor cell

proliferation factors FGF-2, IGF-1, and VEGF exhibit early decline during the course of aging in the hippocampus: role of astrocytes. *Glia* **51**, 173-186.

Simon, D. K., Prusky, G. T., O'Leary, D. D. and Constantine-Paton, M. (1992). *N*-methyl-D-aspartate receptor antagonists disrupt the formation of a mammalian neural map. *Proc. Natl. Acad. Sci. USA* **89**, 10593-10597.

Son, H., Yu, I. T., Hwang, S. J., Kim, J. S., Lee, S. H., Lee, Y. S. and Kaang, B. K. (2003). Lithium enhances long-term potentiation independently of hippocampal neurogenesis in the rat dentate gyrus. *J. Neurochem*. **85**, 872-881.

Tashiro, A., Sandler, V. M., Toni, N., Zhao, C. and Gage, F. H. (2006). NMDA-receptor-mediated, cell-specific integration of new neurons in adult dentate gyrus. *Nature* **442**, 923-933.

Tozuka, Y., Fukuda, S., Namba, T., Seki, T. and Hisatsune, T. (2005). GABAergic excitation promotes neuronal differentiation in adult hippocampal progenitor cells. *Neuron* **47**, 803-815.

Wada, T., Haigh, J. J., Ema, M., Hitoshi, S., Chaddah, R., Rossant, J., Nagy, A. and van der Kooy, D. (2006). Vascular endothelial growth factor directly inhibits primitive neural stem cell survival but promotes definitive neural stem cell survival. *J. Neurosci*. **26**, 6803-6812.